Malaysian Journal of Chemistry, 2025, Vol. 27(1), 92-101
(Special Issue: *International Conference on Natural Products, ICNP 2024*)

Synthesis of Benzhydrol-type Derivatives as Stable 1′-Acetoxychavicol Acetate Analogues, Cytotoxic Evaluation and Molecular Docking Study

Mohamad Nurul Azmi[1]*, Kok Hoong Leong[2], Muhammad Solehin Abd Ghani[1], Nur Farah Atiqah Azmi[1], Mohammad Tasyriq Che Omar[3] and Khalijah Awang[4]
[1]Natural Products and Organic Synthesis Research Laboratory (NPSO), School of Chemical Sciences, Universiti Sains Malaysia, 11800 Minden, Penang, Malaysia
[2]Department of Pharmaceutical Chemistry, Faculty of Pharmacy, University of Malaya, 50603 Kuala Lumpur, Malaysia
[3]Biological Section, School of Distance Education, Universiti Sains Malaysia, 11800 Minden, Penang, Malaysia
[4]Department of Chemistry, Faculty of Science, University of Malaya, 50603 Kuala Lumpur, Malaysia
*Corresponding author (e-mail: mnazmi@usm.edu.my)

Four benzhydrol analogues were synthesised, characterised and evaluated for their cytotoxic activity against two human lung carcinoma cell lines (H1975 and A549), and one colorectal carcinoma cell line (HCT116). Compound **3b** (IC_{50} = 5.9 µM) and **3c** (IC_{50} = 9.9 µM) show a good cytotoxic potency on H1975 cell line compared with gefitinib as a positive control (IC_{50} = 56.2 µM). Molecular docking was done to understand the interactions between ligand and the Nuclear Factor-KappaB Kinase alpha (IκBα) protein. These findings suggest that the benzhydrol analogues, particularly **3b** and **3c**, show a promising potential as anticancer agents.

Keywords: Benzhydrol-type analogues; 1′-Acetoxychavicol acetate (ACA); Cytotoxic; MTT assay; Molecular Docking; IκBα protein

Received: August 2024; Accepted: November 2024

Cancer, a multifaceted disease characterised by uncontrolled cell proliferation and metastasis, remains as one of the leading causes of morbidity and mortality worldwide [1]. According to the International Agency for Research on Cancer (IARC), there were almost 20 million new cases of cancer in 2022, along with 9.7 million deaths. Lung cancer was the most frequently diagnosed cancer in 2022, accounting for almost 2.5 million new cases, or one in eight cancers worldwide (12.4% of all cancers globally), followed by cancers of the female breast (11.6%), colorectum (9.6%), prostate (7.3%), and stomach (4.9%). Lung cancer was also the leading cause of cancer death, with around 1.8 million fatalities (18.7%), followed by colorectal (9.3%), liver (7.8%), female breast (6.9%), and stomach (6.8%) cancers [2]. This global health crisis is also reflected in Malaysia, where cancer is the fourth leading cause of death, increasing from 10.5% in 2021 to 12.6% in 2022, according to the Department of Statistics Malaysia (DOSM) 2023 report [3]. Despite extensive efforts to combat this disease, incidence rates continue to rise, underscoring the urgent need for more effective therapeutic strategies.

Previously, cancer treatment options have been limited to surgery, radiation therapy, and chemotherapy, either as single treatments or in combination [4-5]. Although these conventional treatments have been the cornerstone of cancer therapy, they are often hindered by limitations such as drug resistance and adverse side effects. Cancer cells frequently develop mechanisms to evade these treatments, reducing their efficacy over time [6]. Additionally, these treatments can harm healthy cells, leading to side effects like nausea, fatigue, and increased infection risk, which can limit the treatment's dosage and effectiveness [7]. These challenges highlight the necessity to focus on discovering new compounds with potential anticancer properties [8].

One promising source of such compounds is *Alpinia galanga* (L.) Willd., commonly referred as "Greater galangal" [9]. *Galangal*, a well-known spice resembling ginger from the Zingiberaceae family, is widely cultivated in Southeast Asia. Its rhizomes are extensively used as a flavouring agent in traditional cuisine and serve as a remedy for gastrointestinal diseases in traditional Chinese medicine. Based on the phytochemical studies, *A. galanga* contains a diverse range of phenylpropanoids, with 1'-acetoxychavicol acetate (ACA) being the predominant component while most of the pharmacological studies of *A. galanga* also have focused primarily on ACA [10] (Figure 1). ACA exhibited a wide range of bioactivities including anti-inflammatory, anticancer, antiviral, antimicrobial, antioxidant, antiallergic, and gastroprotective activities [11] (Figure 1).

†Paper presented at the International Conference on Natural Products 2024 (ICNP 2024)

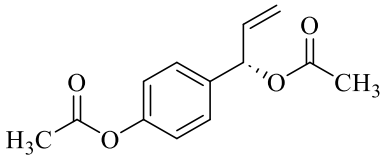

Figure 1. 1′-acetoxychavicol acetate (ACA).

From our prior studies, we had extracted 1'-acetoxychavicol acetate (ACA) from *Alpinia conchigera* Griff, a species of wild ginger found in Malaysia. We discovered that ACA had shown its substantial cytotoxic activity on a variety of cancer cell lines, such as MDA-MB-231 (4.8 μM), MCF-7 (30.0 μM), RT-112 (14.1 μM), EJ-28 (8.2 μM), PC-3 (26.7 μM), HSC-2 (5.0 μM), HSC-4 (5.5 μM), HepG2 (18.0 μM), and CaSki (17.0 μM) [12-13]. Despite the promising cytotoxic activity of ACA, several limitations hinder its therapeutic potential. ACA exhibits suboptimal pharmacokinetic properties, including poor bioavailability and chemical instability, which pose challenges in its formulation and storage. These limitations necessitated the development of more stable and potent analogues. Building on those findings, our latest study has developed stable and more potent cytotoxic compounds by structurally modifying the ACA structure, resulting in benzhydrol analogues. These benzhydrol analogues exhibited significant cytotoxic activity specifically against human breast cancer cell lines MCF-7 and MDA-MB-231 [14]. Furthermore, molecular docking studies showed strong binding affinity to the Nuclear Factor-KappaB Kinase alpha (IκBα) protein, with binding energies ranging from -5.13 and -7.27 kcal/mol, indicating their potential as efficacious anticancer agents.

The IκBα protein plays a critical role in the regulation of the NF-κB signaling pathway, which is involved in the control of cell survival, immune responses and inflammation [15,16]. IκBα binds to NF-κB, preventing its activation inside the cytoplasm. When cellular signals trigger its degradation, NF-κB translocate to the nucleus to activate specific target genes [16]. Various cancers, including breast cancer, often constitutively activate NF-κB, leading to tumour growth and resistance to apoptosis [17]. Therefore, targeting IκBα in molecular docking studies are necessary due to its association with illnesses such as cancer and chronic inflammation. By targeting IκBα, our newly developed benzhydrol analogues can inhibit the NF-κB pathway, thereby suppressing cancer cell proliferation and inducing apoptosis. This mechanism makes IκBα an attractive target for anticancer therapy, as inhibiting its function can effectively disrupt cancer cell survival mechanisms.

In this paper, we aim to further explore the therapeutic potential of these benzhydrol analogues by synthesising new compounds and evaluating the cytotoxicity of the compounds on the human lung carcinoma cell lines H1975 and A549, and the colorectal carcinoma cell line HCT116. The molecular docking of potent compounds on IκBα were studied to understand their interactions between the ligand and active sites.

EXPERIMENTAL

Generals

All reactions were carried out in heat-dried glassware under an atmosphere of nitrogen unless otherwise stated. All liquid transfers were conducted using standard syringe or cannula techniques. DCM was dried under molecular sieves 4Å. All other reagents were obtained from Merck or Aldrich and used as received. Column chromatography was performed on silica gel (Merck, 60 Å C. C. 40-63 mm) as the stationary phase. Thin Layer Chromatography (TLC) was performed on alumina plates pre-coated with silica gel (Merck silica gel, 60 F254), which were visualized by the quenching of UV fluorescence when applicable (λ_{max} = 254 nm and/or 366 nm) and/or by spraying with vanillin in acidic ethanol followed by heating with a heat gun. NMR spectra were recorded on a Bruker Avance (500 MHz for ^{1}H NMR, 125 MHz for ^{13}C NMR) spectrometer system. Data were analysed via TopSpin 3.6.1 software package. Spectra were referenced to TMS or residual solvent ($CDCl_3$ = 7.26 ppm in ^{1}H spectroscopy, and 77.0 ppm in ^{13}C spectroscopy; MeOD-D_4 = 4.78, 3.31 ppm in ^{1}H spectroscopy, and 49.2 ppm in ^{13}C spectroscopy). Fourier transform infrared (FT-IR) spectra were recorded by Perkin Elmer FT-IR spectroscopy (Perkin Elmer, Waltham, MA, USA) in the frequency range of 4000 – 400 cm^{-1} using the ATR method.

Methodology

*Synthesis of 4-(hydroxy(phenyl)methyl)phenol (**2**)*

The 4-hydroxybenzophenone (**1**) (2.13 g, 10.76 mmol) was treated with $NaBH_4$ (1.59 g; 4 equiv.) in the mixture of THF (100 mL) and H_2O (30 mL). While the mixture was heated under reflux overnight, the colour of the mixture gradually changed from pale yellow to colourless. The reaction mixture was quenched with saturated aqueous ammonium chloride (NH_4Cl) (20 mL). The layers were then separated, and the aqueous layer was extracted with ethyl acetate (EtOAc) (3×20 mL). The combined organic solvents were then dried over sodium sulphate (Na_2SO_4), filtered, and collected. The product was directly used

without further purification. The spectroscopic data will compare with those reported in the literature (Supporting information, S1-S2). White solid. Yield: (2.14 g, 99%). IR ($\tilde{\nu}$/cm^{-1}): ^{1}H NMR (500 MHz, CD_3OD, δ/ppm): 4.48 (br s, 1H, O-H), 5.63 (s, 1H, H-7), 6.69 (d, *J*= 8.6 Hz, 2H, H-3, H-5), 7.09 (d, *J*= 8.6 Hz, 2H, H-2, H-6), 7.14 (t, *J*= 7.5 Hz, 1H, H-11), 7.24 (t, *J*= 7.5 Hz, 2H, H-10, H-12), 7.28 (d, *J*= 7.5 Hz, 2H, H-9, H13). ^{13}C NMR (125 MHz, CD_3OD, δ/ppm): 76.8 (C-7), 116.1 (C-3, C-5), 127.7 (C-9, C13), 128.1 (C-11), 129.3 (C-2, C-6, C-10, C-12), 137.0 (C-1), 146.4 (C-8), 157.9 (C-4).

*Synthesis of Benzhydrol Analogues **3a-3d***

A benzhydrol **2** (~0.220 g; 1.0 equiv.) was dissolved in 20 mL of dry dichloromethane (DCM) and stirred in an ice bath. The 4-dimethylaminopyridine (DMAP) (0.1 equiv.), triethylamine (Et_3N) (0.5 equiv.) and acyl chloride (2.2 equiv.) were added dropwise while stirring the reaction solution. The ice bath was removed and the mixture was allowed to stirred at room temperature for overnight. The reaction progress was monitored by TLC (1:4, *n*-hexane: ethyl acetate). After stirring at room temperature for overnight, the reaction mixture was quenched with saturated aqueous ammonium chloride (NH_4Cl) (20 mL). The layers were then separated and the aqueous layer was extracted with ethyl acetate (EtOAc) (3×20 mL). The combined organic solvents were then dried over sodium sulphate (Na_2SO_4), filtered, and collected. The solvent was removed under reduced pressure by using a rotary evaporator then gave the product **3** (Supporting information, S5-S14).

*4-((benzoyloxy)(phenyl)methyl)phenyl benzoate (**3a**)*: A benzhydrol **2** (0.212 g, 1.06 mmol) was dissolved in 10 mL of dry dichloromethane (DCM) and stirred in an ice bath. The 4-dimethylaminopyridine (DMAP) (0.268 g, 2.20 mmol), triethylamine (Et_3N) (0.31 mL, 2.22 mmol) and benzyl chloride (0.26 mL, 2.20 mmol) were added dropwise while stirring the reaction solution. The reaction then proceeded and worked up according to the general procedure. White solid. Yield: (0.38 g, 85%). IR ($\tilde{\nu}$/cm^{-1}): 3021 (sp2 C-H stretching), 1725 (C=O stretching), 1211 (C-O stretching). ^{1}H NMR (500 MHz, $CDCl_3$, δ/ppm): 7.08 (s, 1H, H-7), 7.14 (d, *J*= 8.7 Hz, 2H, H-3, H-5), 7.23 (t, *J*= 7.3 Hz, 1H, H-11), 7.30 (t, *J*= 7.3 Hz, 2H, H-10, H-12), 7.38-7.44 (m, 8H, H-2, H-6, H-9, H-13, H-4', H-6', H-4″, H-6″), 7.51 (t, *J*= 7.3 Hz, 1H, H-5″), 7.55 (t, *J*= 7.3 Hz, 1H, H-5'), 8.08 (d, *J*= 8.5 Hz, 2H, H-3″, H-7″), 8.11 (d, *J*= 8.5 Hz, 2H, H-3', H-7'). ^{13}C NMR (125 MHz, $CDCl_3$, δ/ppm): 76.9 (C-7), 121.8 (C-3, C-5), 127.2 (C-9, C-13), 128.1 (C-11), 128.5 (C-4', C-6', C-4″, C-6″), 128.6 (C-2, C-6), 128.6 (C-10, C-12), 129.4 (C-2″), 129.8 (C-3″, C-7″), 130.1 (C-2'), 130.2 (C-3', C-7'), 137.9 (C-1), 140.0 (C-8), 150.6 (C-4), 165.1 (C-1'), 165.6 (C-1").

*4-((isobutyryloxy)(phenyl)methyl)phenyl isobutyrate (**3b**)*: A benzhydrol **2** (0.220 g, 1.10 mmol) was dissolved in 20 mL of dry dichloromethane (DCM) and stirred in an ice bath. The 4-dimethylaminopyridine (DMAP) (0.268 g, 2.20 mmol), triethylamine (Et_3N) (0.31 mL, 2.22 mmol) and isobutyryl chloride (0.23 mL, 2.20 mmol) were added dropwise while stirring the reaction solution. The reaction then proceeded and worked up according to the general procedure. Yellowish oil. Yield: (0.32 g, 86%). IR ($\tilde{\nu}$/cm^{-1}): 2995 (sp2 C-H stretching), 1735 (C=O stretching), 1504, 1461, 1195 (C-O stretching), 1151, 750. ^{1}H NMR (500 MHz, $CDCl_3$, δ/ppm): 1.20 (d, *J*= 7.0 Hz, 6H, H-3″, H-4″), 1.30 (d, *J*= 7.0 Hz, 6H, H-3′, H-4′), 2.66 (m, 1H, H-2″), 2.78 (m, 1H, H-2′), 6.86 (s, 1H, H-7), 7.04 (d, *J*= 8.6 Hz, 2H, H-3, H-5), 7.27-7.35 (m, 7H, H-2, H-6, H-9–H-13). ^{13}C NMR (125 MHz, $CDCl_3$, δ/ppm): 18.8 (C-3′, C-4′), 18.9 (C-3″, C-4″), 34.1 (C-2′), 34.2 (C-2″), 76.0 (C-7), 121.5 (C-3, C-5), 127.0 (C-9, C-13), 127.9 (C-11), 128.2 (C-2, C-6), 128.5 (C-10, C12), 137.8 (C-1), 140.1 (C-8), 150.4 (C-4), 175.5 (C-1'), 175.9 (C-1").

*4-((pentanoyloxy)(phenyl)methyl)phenyl pentanoate (**3c**)*: A benzhydrol **2** (0.220 g, 1.10 mmol) was dissolved in 20 mL of dry dichloromethane (DCM) and stirred in an ice bath. The 4-dimethylaminopyridine (DMAP) (0.268 g, 2.20 mmol), triethylamine (Et_3N) (0.31 mL, 2.22 mmol) and valeroyl chloride (0.24 mL, 2.20 mmol) were added dropwise while stirring the reaction solution. The reaction then proceeded and worked up according to the general procedure. Yellowish oil. Yield: (0.30 g, 74%). IR ($\tilde{\nu}$/cm^{-1}): 3021 (sp2 C-H stretching), 2932 (Csp3-H stretching), 1728 (C=O stretching), 1507, 1450, 1209 (C-O stretching), 1160, 746. ^{1}H NMR (500 MHz, $CDCl_3$, δ/ppm): 0.81 (t, J= 7.4 Hz, 3H, H-5″), 0.87 (t, J= 7.4 Hz, 3H, H-5'), 1.25 (m, 2H, H-4″), 1.35 (m, 2H, H-4'), 1.57 (m, 2H, H-3″), 1.64 (m, 2H, H-3'), 2.33 (t, J= 7.7 Hz, 2H, H-2″), 2,45 (t, J= 7.6 Hz, 2H, H-2'), 6.81 (s, 1H, H-7), 6.97 (d, J= 8.6 Hz, 1H, H-3, H-5), 7.15-7.25 (m, 7H, H-2, H-6, H-9–H-13). ^{13}C NMR (125 MHz, $CDCl_3$, δ/ppm): 13.7 (C-5′), 13.7 (C-5″), 22.2 (C-4′, C-4″), 27.0 (C-3′, C-3″), 34.1 (C-2′), 34.3 (C-2″), 76.0 (C-7), 121.6 (C-3, C-5), 127.1 (C-9, C-13), 128.0 (C-11), 128.3 (C-2, C-6), 128.5 (C-10, C12), 137.8 (C-1), 140.1 (C-8), 150.3 (C-4), 172.2 (C-1'), 172.7 (C-1").

*4-(((furan-2-carbonyl)oxy)(phenyl)methyl)phenyl furan-2-carboxylate (**3d**)*: A benzhydrol **2** (0.220 g, 1.10 mmol) was dissolved in 20 mL of dry dichloromethane (DCM) and stirred in an ice bath. The 4-dimethylaminopyridine (DMAP) (0.268 g, 2.20 mmol), triethylamine (Et_3N) (0.31 mL, 2.22 mmol) and 2-furoyl chloride (0.22 mL, 2.20 mmol) were added dropwise while stirring the reaction solution. The reaction then proceeded and worked up according to the general procedure. Brown solid. Yield: (0.35 g, 82%). IR ($\tilde{\nu}$/cm^{-1}): 3024 (sp2 C-H stretching), 1725 (C=O stretching), 1513, 1473, 1214 (C-O stretching), 1174. ^{1}H NMR (500 MHz, $CDCl_3$, δ/ppm): 6.53 (dd, *J*= 3.5, 1.6 Hz, 1H, H-3'), 6.59 (dd, *J*= 3.6, 1.6 Hz, 1H, H-4'), 6.61 (dd, *J*= 3.5, 1.6 Hz, 1H, H-5'), 7.12 (s, 1H,

H-7), 7.21 (d, *J*= 8.5 Hz, 2H, H-3, H-5), 7.31 (t, *J*= 8.2 Hz, 1H, H-11), 7.37 (t, *J*= 8.2 Hz, 2H, H-10, H-12), 7.42 (d, *J*= 8.2 Hz, 2H, H-9, H-13), 7.46 (d, *J*= 8.5 Hz, 2H, H-2, H-6), 7.61 (d, *J*= 0.7 Hz, 1H, H-3″), 7.67 (d, *J*= 0.7 Hz, 1H, H-4″), 7.71 (d, *J*= 0.7 Hz, 1H, H-5″). ^{13}C NMR (125 MHz, $CDCl_3$, δ/ppm): 76.6 (C-7), 111.9 (C-3'), 112.3 (C-4'), 112.7 (C-5'), 121.7 (C-3, C-5), 127.2 (C-9, C-13), 128.2 (C-11), 128.5 (C-2, C-6), 128.6 (C-10, C12), 137.8 (C-1), 139.5 (C-8), 143.9 (C-2'), 144.5 (C-2″), 146.8 (C-3″), 147.3 (C-4″), 148.6 (C-5″), 149.9 (C-4), 156.8 (C-1'), 157.7 (C-1″).

Biological Assay

Cell Culture

Three human cancer cell lines, A549 cell line (human lung cancer with wild-type EGFR), H1975 cell line (human lung cancer with L858R/T970M double EGFR mutations) and HCT116 cell line (human colon cancer with G13D KRAS mutation) were obtained from American Type Culture Collection (ATCC), USA. Complete DMEM culture media supplemented with 10% heat-inactivated FBS and 2 mM L-glutamine (Sigma-Aldrich, MO., USA) was used to culture all the cancer cell lines in a cell incubator (Thermo Fisher Scientific Inc., MA, USA) at 37 °C with a humidified atmosphere of 5% CO_2 [18].

Cytotoxic Evaluation of Benzhydrol Analogues

Cytotoxic evaluation of the benzhydrol analogues was evaluated using the standard MTT assay. The benzhydrol analogues were dissolved in DMSO and serially diluted with complete DMEM to 0.4 – 100 µM concentration, ensuring the DMSO is below 0.5% v/v. The positive controls, Gefitinib for lung cancer cell lines and Cisplatin for colon cancer cell line solutions were also prepared in the same manner as the benzhydol analogues. A total of $8x10^3$ cells per well were seeded into 96-well microplate in complete DMEM culture media and cultured in the cell incubator for 24 hours. Then, the culture media were refreshed with culture media containing the benzhydrol analogues or drug standards in triplicates and incubated in the cell incubator for 24 hours. After 24 hours, 20µL of 5mg/mL MTT reagent was added and incubated in the cell incubator for another 3 hours. The formed formazan crystal was dissolved in 100 µL DMSO and the absorbance was measured using a microplate reader (Tecan Infinite M200, Tecan Group Ltd., Mannedorf, Switzerland) at 570nm wavelength. The IC_{50} of the drug standards and benzhydrol analogues were determined from dose response curves using Prism 8.0.2 software (GraphPad Software Inc., CA, USA) [19,20].

Molecular Docking Studies

The structures of the target compounds were sketched using ChemDraw Professional 22.0 software package (Revvity Signals Software, MA, USA). Using the Chem3D hotlink add-in in this software, the structure of these compounds was converted into a three-dimensional (3D) representation, the energy was minimised using the MM2 force field and saved as .pdb files. The target compounds are then further prepared using the Dock Prep tools of UCSF Chimera 1.17 (Regents of University of California, CA, USA) by adding polar hydrogen, calculating the Gasteiger charge, defining and selecting the torsion tree of the ligand, and later saved as .pdbqt files. The inhibitory protein, known as I-Kappa-B Alpha/NF-Kappa-B complex (IκBα) with PDB ID: 1NFI, was downloaded from the RCSB Protein Data Bank website (www.rcsb.org). The water molecules, unrelated heteroatoms, chain A, chain B, chain C, chain E, and chain F of this protein were removed using the Dock Prep tools in UCSF Chimera. The protein was then subjected to minimisation by steepest descent steps followed by the addition of polar hydrogen atoms, Kollman charges and solvation parameters. The prepared protein was saved in .pdbt format. The molecular docking simulation was performed by AutoDock Vina to analyse the binding energy and binding interactions between the target compounds and prepared protein. The grid box size were set at 27.0 × 38.0 × 39.0 (x, y, z) with grid centre coordinates of -5.9, 81.0 and 59.0 (x, y and z), covering the location of the protein at chain D where the N-terminal of IκBα residues interact with NF-κB molecules [14]. The active interactions of protein and compounds was analysed and visualised for their 2D and 3D conformations using BIOVIA Discovery Studio Visualizer 2024 (Dassault Systems, CA, USA).

RESULTS AND DISCUSSION

Synthesis of Benzhydrol Analogues

Scheme 1 shows the route for the preparation of four benzhydrol analogues **3a-3d**. The benzyhydrol analogues were synthesised from the intermediate **2**, which was prepared from reduction of 4-hydroxybenzophenone (**1**) using sodium borohydride (Scheme 1). Treatment of **2** with respective acyl chloride in the presence of triethylamine and dimethyl-aminopyridine (DMAP) at 0˚C afforded products between 86-74% yield. All synthesised compounds were elucidated using spectroscopic methods.

Cytotoxic Evaluation

The cytotoxicity evaluation was performed on wild-type EGFR (A549) and L858R/T970M double mutated EGFR (H1975) lung cancer cell lines, as well as G13D KRAS mutated colon cancer cell line. Although ACA has a comparable cytotoxicity (IC_{50} H1975 = 63.3 ± 3.5µM and A549 = 80.1 ±3.8 µM) with the drug Gefitinib (IC_{50} H1975 = 56.2 ± 1.6µM and IC_{50} A549 = 74.9 ±1.4 µM), compound **3b** (IC_{50} = 5.9 ± 0.2µM) and **3c** (IC_{50} = 9.9 ± 0.4µM) were significantly more cytotoxic than Gefitinib in H1975 cancer cell line.

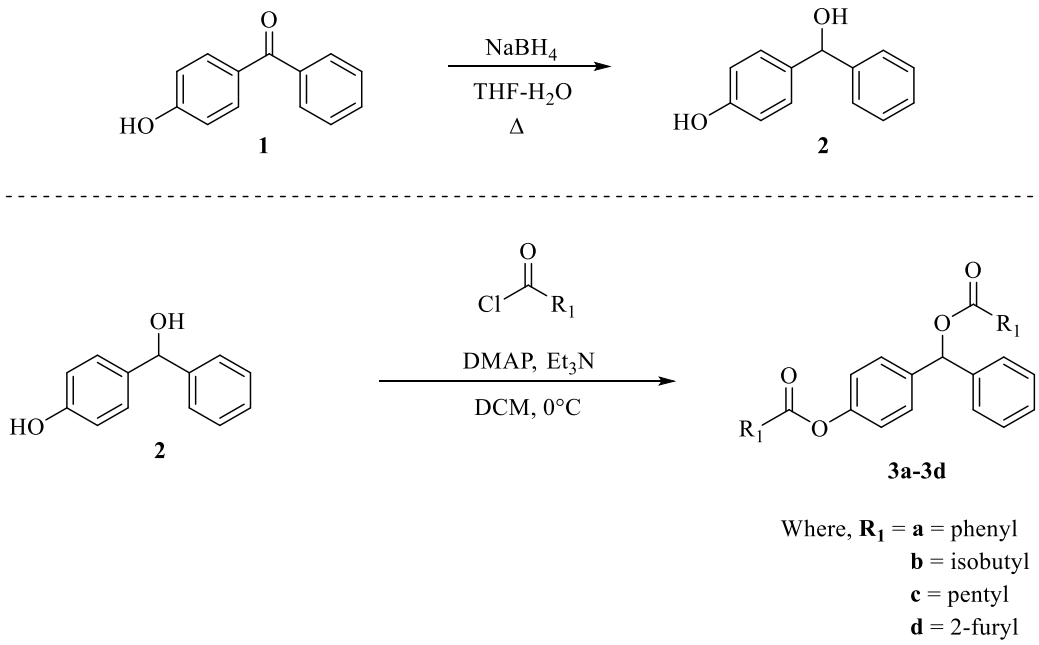

Scheme 1. The preparation of benzhydrol-type analogues **3a**-**3d**.

However, only compound **3a** was more cytotoxic than Gefitinib in the wild-type EGFR lung cancer cell line (A549). This suggest that both compounds **3b** and **3c** are more potent towards the double mutated EGFR lung cancer cell line (H1975). On the other hand, none of the derivates are more cytotoxic than the drug Cisplatin in the KRAS mutated colon cancer cell line. This may also point out that the compounds may not be targeting the KRAS albeit further mechanistic pathway is needed to confirm this. However, modification of the parent ACA into the different derivatives (**3a**-**3d**) did increase the cytotoxicity towards the KRAS mutated colon cancer cell line (HCT116). In general, the addition of bulky groups (such as phenyl, **3a** and 2-furyl, **3d**) displayed less cytotoxicity in H1975 and HCT116 cells, whereas straight chain substituents (isobutyl, **3b** and pentyl, **3c**) showed improved cytotoxicity. However, the cytotoxic effect of the substituents is contrasting in A549 cells. Since the different cancer cell lines have different mutations, the reason behind such contrasting effects between cell lines needs further exploration via EGFR and KRAS receptor binding assays [21,22]. In the aspect of molecular docking, compounds **3b** and **3c** showed good binding affinity towards IκBα. However, the NF-κB is downstream of the EGFR and based on the lung cancer cell lines, the double mutated EGFR (H1975) showed pronounced cytotoxicity. This may indicate that the double mutated EGFR have hyperactivated NF-κB activity and both compounds may have subdued the NF-κB expression leading to higher cytotoxicity observed in H1975 cells compared to wild-type EGFR cells (A549 and HCT116), albeit further mechanistic study is warranted [22].

Table 1. IC_{50} value for benzyhydrol analogues **3a**-**3d**.

Compound	Cytotoxic activity IC_{50} µM (Mean ± SD)		
	H1975	**A549**	**HCT116**
3a	46.6 ± 1.4	65.6 ± 0.9	> 200
3b	5.9 ± 0.2	142.8 ± 2.1	24.7 ± 1.0
3c	9.9 ± 0.4	135.2 ± 0.8	52.8 ± 1.7
3d	24.3 ± 0.9	84.4 ± 1.9	56.8 ± 1.3
ACA	63.3 ± 3.5	80.1 ± 3.8	85.4 ± 3.5
Gefitinib (control)	56.2 ± 1.6	74.9 ± 1.4	-
Cisplatin (control)	-	-	19.6 ± 0.4

Results are expressed as mean ± standard deviation (SD) (*n*=3) of at least three independent experiments.

Molecular Docking Studies

Molecular docking analysis was performed using the AutoDock Vina programme to extend our understanding of the binding affinities and modes of interaction between the most potent ACA analogues in cytotoxicity evaluation of H1975 lung cancer cell lines and the N-terminal residue of IκBα (PDB ID: 1NFI) [14, 23, 22]. This N-terminal region plays a crucial role in regulating the activity of nuclear factor-kappa B (NF-κB), a transcription factor involved in immune responses, inflammation, cell proliferation and apoptosis [25, 26]. Targeting these N-terminal residues may allow modulation of NF-κB activity, which may have an impact on cancer cell behaviour [25, 26]. The molecular docking results of the potent compounds with the key protein are indicated by their binding energy and binding interactions, which are listed in Tables 2 and 3.

Table 2. *In silico* binding energy of related ACA analogues and gefitinib with N-terminal residue of IκBα protein.

Protein	Compound	Binding energy (kcal mol^{-1})
IκBα (PDB ID: 1NFI)	**3b**	-5.6 ± 0.1
	3c	-5.4 ± 0.1
	Gefitinib (Control)	-6.0 ± 0.1

Results are expressed as mean ± standard deviation (SD) for *n*=3 experiments

Table 3. Binding interactions of compounds **3b**, **3c** and gefitinib with *N*-terminal residue of IκBα protein.

Protein	Compound	Protein residue	Interacting unit of compound	Types of interaction
IκBα (PDB ID: 1NFI)	**3b**	SER76	-C=O	Carbon H-bond
		PHE77	-C=O	H-bond (2.82 Å)
			Phenyl	π-π T-shaped
			-CH_3	π-Sigma
		VAL97	Phenyl	π-Alkyl
		PHE103	Phenyl	π-π Stacked
	3c	LEU70	-CH_2	Alkyl
		PHE77	-CH_2	π-Alkyl
		GLN96	-C=O	H-bond (2.25 Å)
		VAL97	Phenyl	π-Alkyl
		PHE103	Phenyl	π-π Stacked
	Gefitinib (Control)	LEU70	Quinazoline ring	π-Alkyl
		PHE77	3-chloro-4-fluorophenyl ring	π-π Stacked
			-Cl	π-Alkyl
		VAL93	3-chloro-4-fluorophenyl ring	π-Alkyl
		GLN96	-O of morpholin ring	H-bond (2.90 Å)
			-CH_2 of morpholin ring	Carbon H-bond
		ALA102	-CH_3	Alkyl
		PHE103	Quinazoline ring	π-π Stacked
			Quinazoline ring	π-π Stacked
			3-chloro-4-fluorophenyl ring	π-π Stacked
			-CH_3	π-Alkyl

The most potent compounds of **3b** and **3c** were selected for molecular docking analysis, and it is observed that both compounds and the gefitinib control generally have an almost similar binding energy with the protein, ranging from -6.0 to -5.4 kcal mol^{-1}. In particular, **3b** and **3c** have a slightly higher binding energy with the protein compared to gefitinib (-6.0 ± 0.1 kcal mol^{-1}). Compound **3b** exhibited a binding energy of -5.6 ± 0.1 kcal mol^{-1} and formed six types of interactions (Figure 2), starting with a hydrogen bond (2.82 Å) and a carbon-hydrogen bond between the -C=O group of **3b** with PHE77 and SER76 of the protein, respectively. The phenyls of **3b** also showed hydrophobic interactions with PHE77, VAL97 and PHE103 through π-π T-shaped, π-alkyl and π-π stacked interactions, correspondingly. Additionally, a π-sigma interaction was formed between the methyl group of **3b** and PHE77 of the protein residue.

Next, compound **3c** interacted with the protein *via* five types of interactions (Figure 3) with a binding energy of -5.4 ± 0.1 kcal mol^{-1}. The interactions include a hydrogen bond (2.25 Å) between the C=O group of **3c** and GLN96 then an alkyl interaction between the methylene moiety and the LEU70 residues of the protein. In addition, the methylene of **3c** also formed a π-alkyl interaction with the PHE77 residue. A π-alkyl and a π-π stacked interactions were demonstrated between the phenyl group of **3c** and the protein residues of VAL97 and PHE103, respectively. In brief, the positive control gefitinib showed eleven modes of interaction (Figure 4) with the N-terminal of the IκBα protein, the most significant being hydrogen bond (2.90 Å) and carbon hydrogen bond between the oxygen (-O) and methylene moieties of the morpholin ring with the GLN96 residue. Remarkably, GLN96 in IκBα is crucial for the specific binding interaction between IκBα and p65 of NF-κB proteins, which has implications for NF-κB regulation and cellular processes [27, 28].

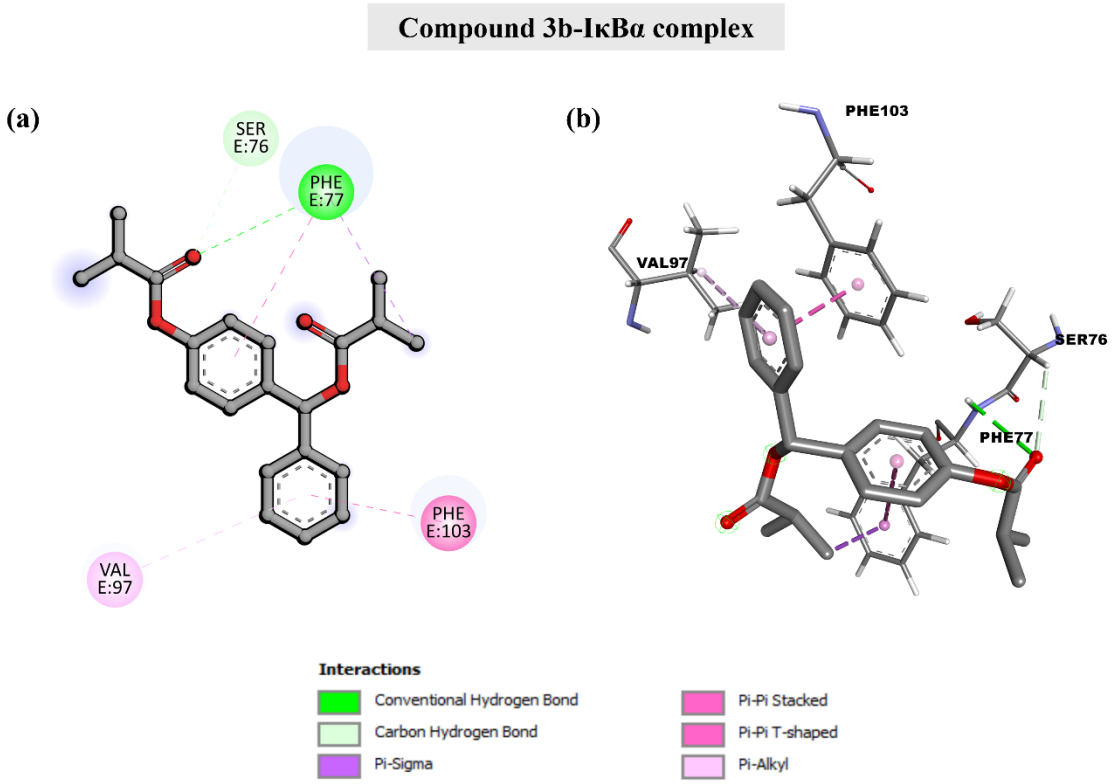

Figure 2. Binding interactions of **3b** and IκBα protein (a) 2D form (b) 3D form.

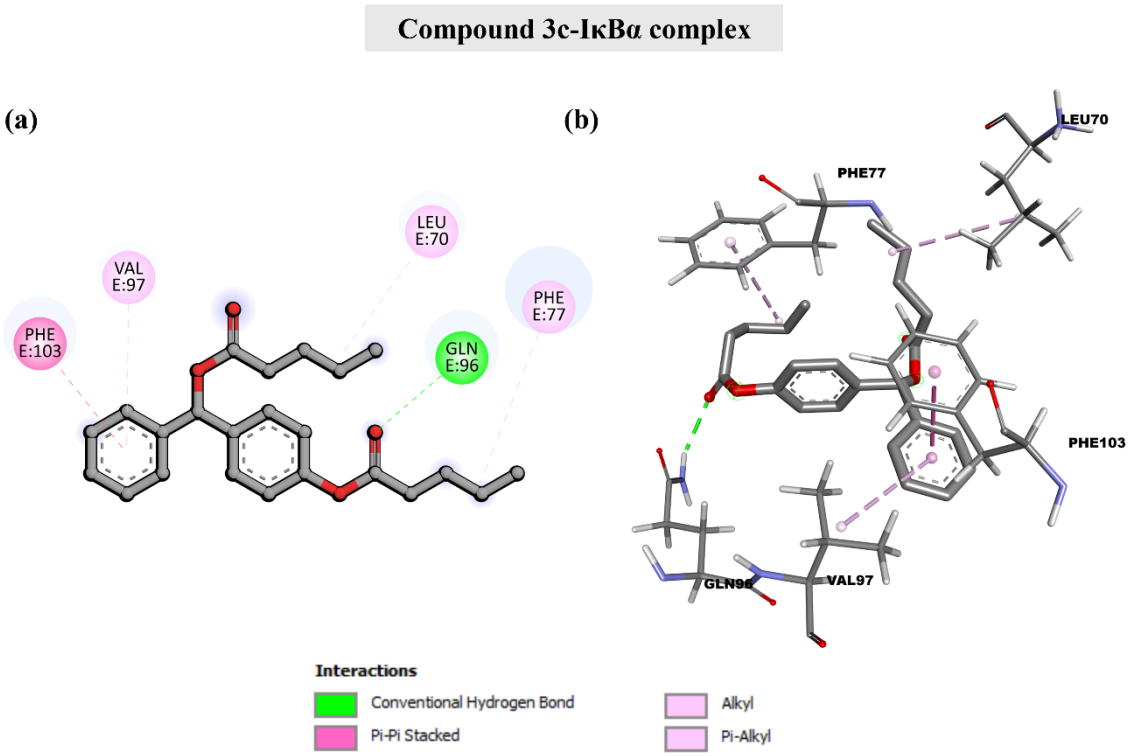

Figure 3. Binding interactions of **3c** and IκBα protein (a) 2D form (b) 3D form.

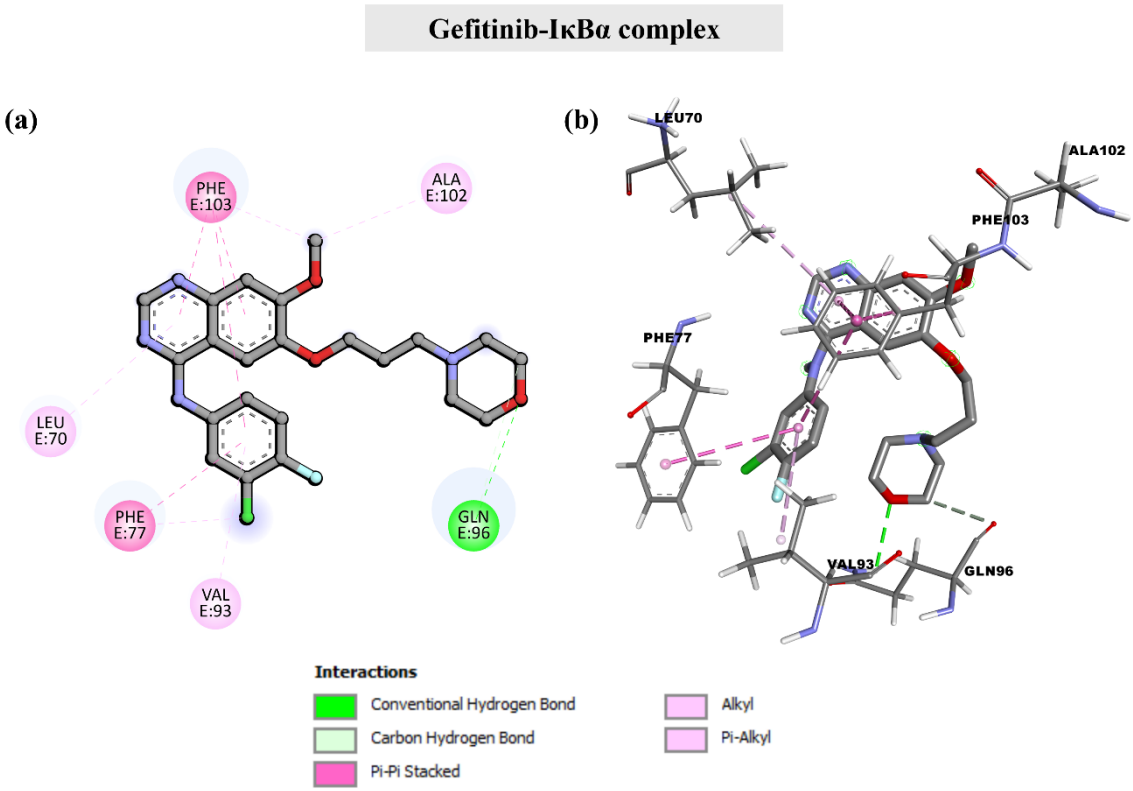

Figure 4. Binding interactions of gefitinib and IκBα protein (a) 2D form (b) 3D form.

CONCLUSION

In summary, the synthesis and characterisation of four benzhydrol analogues, followed by their cytotoxic evaluation, demonstrated that compounds **3b** and **3c** exhibited significant efficacy against the H1975 lung carcinoma cell line surpassing the performance of gefitinib as a positive control. Molecular docking studies indicated crucial interactions between these compounds and nuclear factor kappaB kinase alpha (IκBα) protein. These results suggest that the benzhydrol analogues, especially **3b** and **3c**, have great potential as lead compounds for the development of new anticancer drugs. Future research should focus on detailed mechanistic investigations and *in vivo* studies to fully evaluate their therapeutic potential.

ACKNOWLEDGEMENTS

The author would like to acknowledge the financial support from the Ministry of Higher Education Malaysia (MOHE) under the Fundamental Grant Research Scheme (FRGS) -FRGS/1/2023/STG04/USM/02/3. The authors sincerely thank University Sains Malaysia (USM) for the approval of sabbatical leave for M.N.A. and the NPSO Laboratory for the facilities used in this research work.

REFERENCES

1. Brown, J. S., Amend, S. R., Austin, R. H., Gatenby, R. A., Hammarlund, E. U. & Pienta, K. J. (2023) Updating the definition of cancer. *Molecular Cancer Research*, **21(11)**, 1142–1147.

2. Ferlay, J., Ervik, M., Lam, F., Colombet, M., Mery, L., Piñeros, M., Znaor, A., Soerjomataram, I. & Bray, F. (2024) Global Cancer Observatory: Cancer Today (Version 1.0). *International Agency for Research on Cancer*. Retrieved July 6, 2024.

3. Department of Statistics Malaysia (2023) Statistics on causes of death, Malaysia, 2023. Retrieved July 28, 2024. https://www.dosm.gov.my/uploads/release-content/file_20231030111646.pdf.

4. GlobalSurg Collaborative and National Institute for Health Research Global Health Research Unit on Global Surgery (2021) Global variation in postoperative mortality and complications after cancer surgery: A multicentre, prospective cohort study in 82 countries. *Lancet*, **397**, 387–397.

5. Roy, A. & Li, S. D. (2016) Modifying the tumor microenvironment using nanoparticle therapeutics. *Wiley Interdisciplinary Reviews Nanomedicine and Nanobiotechnology*, **8(6)**, 891–908.

6. Shapira, A., Livney, Y. D., Broxterman, H. J. & Assaraf, Y. G. (2011) Nanomedicine for targeted cancer therapy: Towards the overcoming of drug resistance. *Drug Resistance Update*, **14(3)**, 150–163.

7. Mondal, J., Panigrahi, A. K. & Khuda-Bukhsh, A. R. (2014) Conventional chemotherapy: Problems and scope for combined therapies with certain herbal products and dietary supplements. *Austin Journal of Molecular and Cellular Biology*, **1**, 10.

8. Sasidharan, S., Chen, Y., Saravanan, D., Sundram, K. M. & Yoga Latha, L. (2011) Extraction, isolation and characterization of bioactive compounds from plants' extracts. *African journal of traditional, complementary, and alternative medicines: AJTCAM*, **8(1)**, 1–10.

9. Rao, K., Ch, B., Narasu, L. M. & Giri, A. (2010) Antibacterial activity of *Alpinia galanga* (L) Willd crude extracts. *Applied biochemistry and biotechnology*, **162(3)**, 871–884.

10. Flora Republicae Popularis Sinicae [M] (1981) *Beijing: Science Press*, **16**, 1981: 71.

11. Ajay, G. N. & Vijaykumar, M. K. (2015) Comparative pharmagognostic and phytochemical investigation of two *Alpinia* species from Zingiberaceae family. *World Journal of Pharmaceutical Research*, **4(5)**, 1417–1432.

12. Liew, S. K., Azmi, M. N., In, L. L., Awang, K. & Nagoor, N. H. (2017) Anti-proliferative, apoptotic induction, and 1′*S*-1′-acetoxychavicol acetate analogs on MDA-MB-231 breast cancer cells. *Drug Des Devel Ther*, **11**, 2763–2776.

13. Awang, K., Azmi, M. N., In, L. L., Aziz, A. N., Ibrahim, H. & Nagoor, N. H. (2010) The apoptotic effect of 1´*S*-1´-acetoxychavicol acetate from *Alpinia conchigera* on human cancer cells. *Molecules*, **15**, 8048–8059.

14. Azmi, M. N., Tan, C. S., Abdulameed, H. T., Kamal, N. N. S. N. M., Kahar, N. E. A. & Omar, M. T. C (2024) Synthesis of benzhydrol analogues based on 1-acetoxychavicol acetate (ACA), as a stable and potent antiproliferative agent on breast cancer cell lines, ADMET analysis and molecular docking study. *Organic Communications*, **17(2)**, 99–114.

15. Gupta, S. C., Kim, J. H., Prasad, S. & Aggarwal, B. B. (2010) Regulation of survival, proliferation, invasion, angiogenesis, and metastasis of tumor cells through modulation of inflammatory pathways by nutraceuticals. *Cancer metastasis reviews*, **29(3)**, 405–434.

16. Gilmore, T. D. (2006) Introduction to NF-κB: Players, pathways, perspectives. *Oncogene*, **25(51)**, 6680–6684.

17. Wang, W., Nag, S. A. & Zhang, R. (2015) Targeting the NFκB Signaling Pathways for Breast Cancer Prevention and Therapy. *Current Medicinal Chemistry*, **22(2)**, 264.

18. Tiamas, S. G., Daressy, F., Samra A. A., Bignon, J., Steinmetz, V., Litaudon, M., Fourneau, C., Leong, K. H., Ariffin, A., Awang, K., Desrat, S. & Roussi, F. (2020) Pro-apoptotic carboxamide analogues of natural fislatifolic acid targeting Mcl-1 and Bcl-2. *Bioorganic and Medicinal Chemistry Letters*, **30**, 127003.

19. Abdulwahab, M. K., Tan, K. H., Dzulkeflee, R., Leong, K. H., Heh, C. H. & Ariffin, A. (2021) *In-silico* studies of the antiproliferative activity of new anilinoquinazoline derivatives against NSCLC cells. *Journal of Molecular Structure*, **1228**, 129786.

20. Leong, K. H., Mahdzir, M. A, Din, M. F. M, Awang, K., Tanaka, Y., Kulkeaw, K., Ishitani, T. & Sugiyama, D. (2017) Induction of intrinsic apoptosis in leukaemia stem cells and *in vivo* zebrafish model by betulonic acid isolated from *Walsura pinnata* Hassk (Meliaceae). *Phytomedicine*, **26**, 11–21.

21. Pak, C. & Miyamoto, S. (2014) A new alpha in line between KRAS and NF-κB activation? *Cancer Discovery*, **3(6)**, 613–615.

22. Rasmi, R. R., Sakthivel, K. M. & Guruvayoorappan, C. (2020) NF-κB inhibitors in treatment and prevention of lung cancer. *Biomedicine and Pharmacotherapy*, **130,** 110569.

23. Agu, P. C., Afiukwa, C. A., Orji, O. U., Ezeh, E. M., Ofoke, I. H., Ogbu, C. O., Ugwuja, E. I. & Aja, P. M. (2023) Molecular docking as a tool for the discovery of molecular targets of nutraceuticals in diseases management. *Scientific Reports*, **13(1)**, 1–18.

24. Jacobs, M. D. & Harrison, S. C. (1998) Structure of an IκBα/NF-κB complex. *Cell*, **95(6)**, 749–758.

25. Wang, X., Peng, H., Huang, Y., Kong, W., Cui, Q., Du, J. & Jin, H. (2020) Post-translational modifications of IκBα: The state of the art. *Frontiers in Cell and Developmental Biology*, **8**, 1–15.

26. Bauerle, K. T., Schweppe, R. E. & Haugen, B. R. (2010) Inhibition of nuclear factor-kappa B differentially affects thyroid cancer cell growth, apoptosis, and invasion. *Molecular Cancer*, **9**, 1–13.

27. Basith, S., Manavalan, B., Gosu, V. & Choi, S. (2013) Evolutionary, structural and functional interplay of the IκB family members. *PloS One*, **8(1)**, 1–19.

28. Carrà, G., Ermondi, G., Riganti, C., Righi, L., Caron, G., Menga, A., Capelletto, E., Maffeo, B., Lingua, M. F., Fusella, F., Volante, M., Taulli, R., Guerrasio, A., Novello, S., Brancaccio, M., Piazza, R., & Morotti, A. (2021) IκBα targeting promotes oxidative stress-dependent cell death. *Journal of Experimental & Clinical Cancer Research*, **40**, 1–17.